Titanium Tungsten Coatings for Bioelectrochemical Applications

R. Wierzbicki*, L. Amato*, J. Łopacińska*, A. Heiskanen*, J. Emnéus*,
A. Downard**, K. Baronian***, M. Tenje*, M. Schmidt*, P. Bøggild*, and K. Mølhave*

*DTU Nanotech, Ørsteds Plads 345East, 2800 Kgs. Lyngby, Denmark
**Univ Canterbury, Dept Chem, Christchurch 1, New Zealand
***Univ Canterbury, Sch. Biol. Sci., Christchurch 1, New Zealand
rafal.wierzbicki@nanotech.dtu.dk

ABSTRACT

This paper presents an assessment of titanium tungsten (TiW) coatings and their applicability as components of biosensing systems. The focus is put on using TiW as an electromechanical interface layer between carbon nanotube (CNT) forests and silicon nanograss (SiNG) cell scaffolds. Cytotoxicity, applicability to plasma-enhanced chemical vapor deposition (PECVD) of aligned CNT forests, and electrochemical performance are investigated. Experiments include culturing of NIH3T3 mouse embryonic fibroblast cells on TiW coated silicon scaffolds, CNT growth on TiW substrates with nickel catalyst, and cyclic voltammetric investigation with PBS-buffered potassium hexacyanoferrate (II/III).

Keywords: electrochemistry, carbon nanotubes, titanium tungsten, biosensing

1 INTRODUCTION

Carbon nanotubes, aside from other applications, are of great interest in bioelectrochemical detection. Multiple sensing applications and electrode arrangements have continuously been reported within the last years [1]. Usually, CNT electrodes are formed on flat substrates. However, nanostructured surfaces with controlled roughness are effective scaffolds for cell culturing and tissue interfacing [2]. Proper choice of surface morphology may either promote or impede cellular growth, and thus allow patterned control of these. In our research, we seek for synergy of both technologies: electrochemistry of carbon nanotubes and scaffolding capabilities of nanostructured surfaces. As one of the first steps towards this goal, we need an electric interface layer between the CNTs and the scaffolds. The aim is an electrically conductive conformal coating, which is biocompatible and electrochemically stable.

Titanium tungsten is a chemically stable, mechanically robust, and electrically conductive material. Its thin conformal coatings can be deposited by sputtering, and thus we chose it as a candidate for our application. Additionally, TiW (as well as pure titanium) exhibits an interesting feature of anodic oxidation [3], [4], [5]. Resulting oxide layer is highly resistive and stable. The thickness can be controlled by the applied potential level [3], thus leaving conductive core leads for the electrodes. If feasible, this could be highly advantageous as usually CNT electrodes are being coated with insulation layers of silica [6] or spin coated polymers [7], and this could be avoided and would simplify the system and fabrication process. It needs to be noted that such an electrode with fully exposed (not buried within an isolation layer) vertically aligned CNT forest is prone to collapse due to capillary forces. However, it has been proven that such a process appears during drying of the CNT electrodes, not during the initial wetting, and that critical point drying in CO_2 can revive the wetted CNT forests [8].

2 EXPERIMENTAL METHODS

All the investigated samples were prepared by magnetron sputtering of TiW (10%at.Ti:90%W, Wordentec coater) onto low doped (resistivity 1-20 Ωcm) 4” silicon wafers with either flat or nanostructured surfaces. Nanostructuring of silicon was made by the black silicon method [9] with reactive ion etching (RIE) in STS ICP Advanced Silicon Etcher system using CF_4, SF_6, and O_2 plasma. Nickel deposition was made by e-beam evaporation and gold deposition by thermal evaporation, both in a Wordentec coater system.

2.1 Cell growth

Silicon nanograss wafers were coated with 100 nm of TiW and diced into chips of 10x10 mm^2. NIH3T3 cells were cultured for 72 hrs to obtain an adherent monolayer on the chips and flat Pyrex substrates that were used as a control. NIH3T3 cells were grown in Dulbecco’s modified Eagle’s medium with Glutamax (DMEM; GIBCO Life Technologies), 10% newborn calf serum (NBS; Sigma) and 1% penicillin-streptomycin (P/S; GIBCO Life Technologies). Standard conditions: 37°C and an atmosphere of 5% CO2 were applied. Vybrant™ CM-DiI labeling solution (Molecular Probes) was used for determining the cell viability according to protocol, which was provided by supplier. To visualize fluorescently labeled cells, a Carl Zeiss Axio Imager M1m equipped with an AxioCam Mr.5 camera was employed.

2.2 Carbon nanotube growth

Flat and nanostructured silicon wafers were coated with 100 nm of TiW. No additional diffusion barrier was used. Nickel catalyst was deposited with a nominal thickness of 6 nm. Subsequently, PECVD growth was performed in a 6" Aixtron Black Magic system (6 mTorr N_2, 160 sccm NH_3, 40 sccm C_2H_2, 100 W DC plasma, 750 °C, and 15 min).

2.3 Electrochemistry

Cyclic voltammetry (CV) of 10mM potassium hexacyanoferrate (II/III) in 50mM phosphate buffered saline (pH = 7.02) (PBS) was used to assess electroactivity of the samples. GAMRY Reference 600 potentionstat was used, with a commercial Ag/AgCl (3M KCl) reference electrode, and a coiled platinum wire counter electrode. Working electrode area was defined by an O-ring with 3.75 mm diameter. CV cycles were run at a scan rate of 50 mV/s. 50 consecutive CV cycles were run for each sample to assess stability.

Three types of samples were investigated: (A) TiW on flat Si; (B) Au islet on flat Si/TiW; (C) PECVD-grown forest of aligned CNTs. All TiW coatings had 100 nm nominal thickness. Gold was thermally evaporated (20 nm) through 1.5 mm thick PMMA shadow mask with Ø0.5 mm holes.

3 RESULTS AND DISCUSSION

3.1 Silicon nanograss fabrication

Silicon nanograss scaffolds were investigated with SEM (FEI Quanta 200 FEG) at 45º angle. Silicon formed rippled pyramidal structures, as well as high aspect ratio spikes (Figure 1a). Titanium tungsten conformally coated the nanostructures (Figure 1b), and balled up around surface irregularities (inset of Figure 1b).

3.2 Cell growth

Investigation with fluorescent microscopy reveals good proliferation and cell adhesion to the scaffold substrates with the cells exhibiting extended morphologies. Within a used time frame of 72hrs, no signs of cytotoxicity were observed, i.e. cellular adhesion, spreading and growth proceeded normally, resulting in characteristic cell morphology.

3.3 Carbon nanotube growth

SEM imaging (SEM LEO, 5kV) shows sparse, vertically aligned CNT forests on both flat and nanostructured substrates (Figure 2a). TEM imaging (FEI Tecnai, 80kV, bright field) reveals carbon nanofibre (CNF)

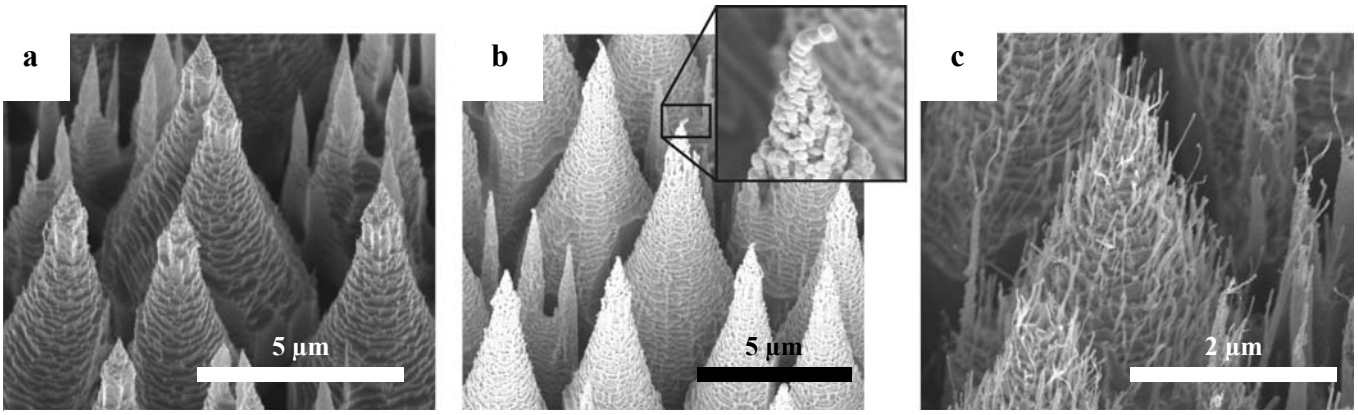

Figure 1: Silicon after treatment with $SF_4/SF_6/O_2$ plasma forms pyramidal and corrugated nanostructures (a). Coating of the formed nanograss with TiW results in a conformal layer (b) balling up on the corrugations (inset). Deposition of nickel catalyst and PECVD processing creates a hierarchical CNTs forest (c).

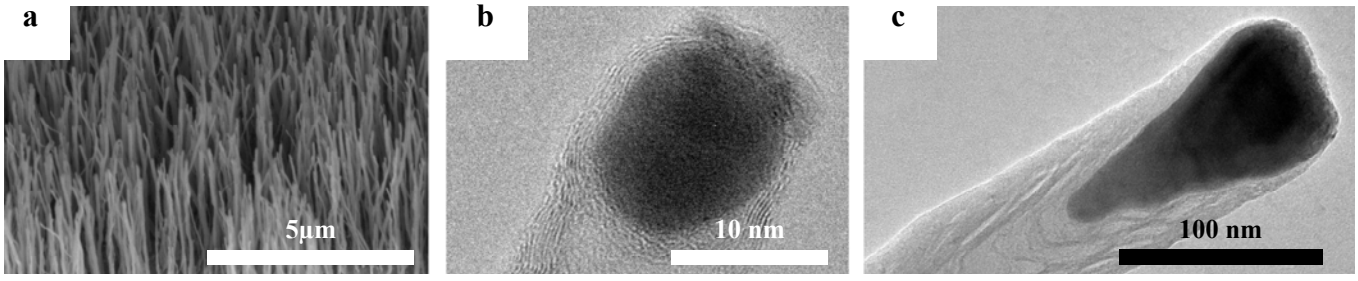

Figure 2: Quality of the fabricated CNT forest was assessed with SEM (a) and TEM (b, c). The forests are vertically aligned with fibres of 20 to 100 nm in diameter. Structure of the tubes is bamboo-like with mostly nanofibres (CNFs) present.

structure (Figures 2b and 2c) which is typical for PECVD grown aligned forests [10]. The process has tip-growth character with nickel catalyst nanoparticles placed at the tops of the fibers.

3.4 Electrochemistry

The CVs of sample A (Figure 3a) show a strong passivation of the TiW coating due to the anodic oxidation. Formation of the insulated layer is nearly instant and the following CVs are stable within most of the potential range, revealing only small passivation for the highest potential.

Sample B passivates in an analogous manner (Figure 3b), however, the gold islet remains electroactive, still providing well defined redox peaks of hexacyanoferrate. Peak separation (ΔE_p) decreases with subsequent CV runs and stabilizes after ca. 20 cycles (Figure 3c). This can be attributed to electrochemical cleaning of the gold. On the other hand, it cannot be attributed to an influence of the TiW anodic oxidation. When an identical sample is passivated by 50 consecutive CV runs in pure 50mM PBS, after switching to the hexacyanoferrate solution the ΔE_p is still not stable. In fact, multiple cycling in hexacyanoferrate is still needed in order to stabilize the ΔE_p.

No significant difference in redox response can be observed for sample C (Figure 3d). Even though the chips are fully covered by the nanotubes, the CNT forests are relatively sparse (Figure 2a) and thus a significant amount of the underlying material is exposed to the electrolyte. Interestingly, the expected anodic oxidation behavior of the underlying material does not occur in the same manner as for sample A. The redox peak of hexacyanoferrate remains unaffected and only a hint of anodic oxidation is given by a drop of a curve tail for higher potentials. This can be explained by nitridation of the TiW, resulting in formation of, for instance, TiWN. Alternatively, it could be explained by conductive amorphous carbon contamination which is created by the PECVD in the absence of the catalyst [10]. The second explanation has been excluded, however, by removing all the carbonous material (including CNTs) in air plasma (50W, 0.6mbar, 2min) and repeating the CV runs of the samples with no observable change.

In order to find out if anodic oxidation of TiWN is possible, additional 50 CV cycles with an increased potential window of -0.4 to +1.5V were run with sample C (Figure 3e). This time, the anodic oxidation was observed and the sample was fully passivated leaving no electroactivity. The full passivation of the CNT electrode can be explained with the oxide layer extending into the CNT-TiW interfaces and undercutting their electric connections (Figure 4).

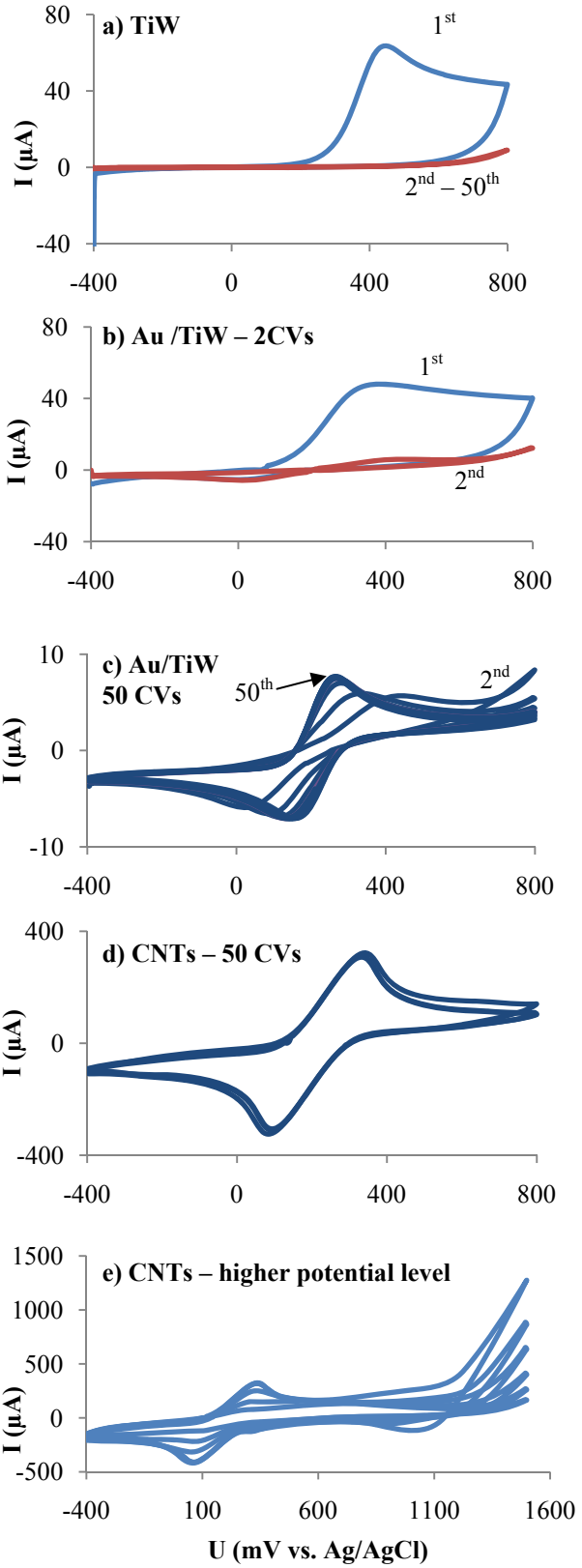

Figure 3: Cyclic voltammograms of: a) pure TiW, b) Au islet on TiW (first two runs), c) Au islet on TiW (runs 2 – 50), d) CNTs on TiW, e) CNTs on TiW, wider potential window. All CVs were made at a rate of 50 mV/s.

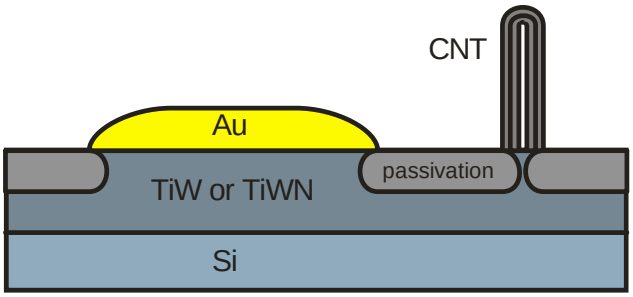

Figure 4: A plausible explanation for full passivation of the CNT forests is a too small aspect ratio between planar features and created oxide thickness. Low aspect ratio results in a full passivation of the electric interfaces between single CNTs.

Unfortunately this prevents us from creation of self-insulated TiW-CNT electrodes with only the CNTs remaining electroactive. It is questionable, whether this would be possible if the nitridation of the TiW could be avoided (e.g. with PECVD using hydrogen as a reducing agent instead of ammonia). As the problem is most likely caused by passivation of the CNT-TiW electric interface, a ratio between CNT average radius and titanium tungsten oxide thickness (created at a given potential) seems to be the crucial factor (Figure 4). The aforementioned gold islet electrode remains active after anodic oxidation, and its radius is at least two to three orders of magnitude larger than the oxidized TiW thickness. This indicates, that forests of CNTs with larger diameters (a couple hundreds of nm) or islets of single-walled carbon nanotubes (SWNTs) which are closely packed [10] could be applied to create self-insulated TiW-CNT electrodes.

4 CONCLUSION AND OUTLOOK

Titanium tungsten proves to be a suitable material for electrically conductive coatings of silicon nanograss scaffolds for cell culturing. It also provides a good diffusion barrier for Ni catalyst and allows growth of electrically connected and vertically aligned CNT forests.

Anodic oxidation of TiW can provide functional self-insulation of an electrode, until the electrode's dimensions are considerably larger than the thickness of the created passivation. This was not the case with the investigated samples, which passivated fully, however modification of CNT forest parameters could solve the problem. Additionally, the presented as-grown hybrid TiWN-CNT electrodes still have a potential for practical applications. An example would be enzymatic detection: CNTs attached to an electroactive non-insulated underlayer, and modified with enzymes have been shown functional in detection of NADH using diaphorase [11].

A closer look on the chemistry of TiW processing in ammonia / acetylene PECVD should be made to directly verify the results. Analytical TEM imaging of the interfaces between a single CNT and the underlayer would help to directly identify the material. Investigation of the nitridation and oxidation dynamics would help optimizing the processes and possibly allowing creation of electrodes with insulated underlayer.

Alternatively, hydrogen-based PECVD growth of CNT forests could be performed, to avoid nitridation of the titanium tungsten and assess if fabrication of CNT electrode structures with anodically insulated surrounding TiW is feasible.

5 ACKNOWLEDGEMENTS

This work was made possible by EU-funded FP7 projects: NANOSCALE (CP-FP 214566-2), TECHNOTUBES (CP-IP 228579-1), and EXCELL (NMP4-SL-2008-214706).

REFERENCES

1. Wang, J., Electroanalysis, 2005. **17**(1): p. 7-14.
2. von der Mark, K., et al., Cell and Tissue Research, 2010. **339**(1): p. 131-153.
3. Blondeau, G., et al., Journal of the Less-Common Metals, 1977. **56**(2): p. 215-222.
4. Habazaki, H., et al., Journal of the Electrochemical Society, 2005. **152**(8): p. B263-B270.
5. Massiani, Y., et al., Thin Solid Films, 1990. **191**(2): p. 305-316.
6. Siddiqui, S., et al., Acs Nano, 2010. **4**(2): p. 955-961.
7. Tu, Y., et al., Electroanalysis, 2005. **17**(1): p. 79-84.
8. Ye, X.R., et al., Journal of Physical Chemistry B, 2006. **110**(26): p. 12938-12942.
9. Jansen, H., et al., Journal of Micromechanics and Microengineering, 1995. **5**(2): p. 115-120.
10. Meyyappan, M., Journal of Physics D-Applied Physics, 2009. **42**(21).
11. Tasca, F., et al., Biosensors & Bioelectronics, 2008. **24**(2): p. 272-278.